Heliyon 9 (2023) e16262

Contents lists available at ScienceDirect

Heliyon

journal homepage: www.cell.com/heliyon

Research article

Effects of changes in land use structure on nitrogen input in the Pingzhai Reservoir watershed, a karst mountain region

Cui Wang [b,c], Zhongfa Zhou [a,b,c,*], Yongliu Li [a,c], Jie Kong [b,c], Hui Dong [a]

[a] School of Karst Science, Guizhou Normal University, Guiyang 550001, China
[b] State Key Laboratory Incubation Base for Karst Mountain Ecology Environment of Guizhou Province, Guiyang 550001, China
[c] School of Geography and Environment, Guizhou Normal University, Guiyang 550001, China

ARTICLE INFO

Keywords:
Karst mountain
Land use
Nitrogen input
Control effect
Water environment

ABSTRACT

Optimizing land use composition to control nitrogen input into water bodies is one way to address surface source pollution in karst mountain regions. In this study, changes in land use, N sources, and spatial and temporal changes of N migration in the Pingzhai Reservoir watershed were evaluated from 2015 to 2021, and the relationship between land use composition and N input was elucidated. N was the main pollution in the water of the watershed; NO_3^- was the dominant form of N, and it did not react during migration. N came from soil, livestock manure or domestic sewage, and atmospheric deposition. Isolating the fractionation effects of source nitrogen is crucial to improve the accuracy of nitrogen and oxygen isotope traceability in the Pingzhai Reservoir. From 2015 to 2021, the grassland area in the Pingzhai Reservoir increased by 5.52%, the woodland area increased by 2.01%, the water area increased by 1.44%, the cropland decreased by 5.8%, unused land decreased by 3.18%, and construction land remained unchanged. Policies and reservoir construction were the main drivers of changes in land-use type in the catchment. Changes in land use structure affected nitrogen input patterns, with unused land having a highly significant positive correlation with inputs of NH_3–N, NO_2^-, and TN, and construction land having a significant positive correlation with the input of NO_2^-. The inhibitory effect of forest and grassland on nitrogen input in the basin was offset by the promoting effect of cropland and construction land on nitrogen input, with unused land becoming a new focus area for nitrogen emissions due to a lack of environmental management. Modifying the area of different land use types in the watershed can effectively control nitrogen input to the watershed.

1. Introduction

The Second National Pollution Source Survey in China found that nitrogen (N) in wastewater and exhaust gas discharged from surface sources of pollution were 18.5 and 1.8 times higher than those from industry, respectively, and are currently the main source of N pollution in Chinese rivers. In karst mountains, total nitrogen emissions from cultivation can account for 32.4% of total regional emissions and 27.38 times more than total industrial emissions (https://www.mee.gov.cn). In the karst mountains, the high and undulating terrain makes N from surface sources of pollution not alleviated [1]. N is the main substance responsible for surface source pollution in karst mountain regions, and also a common pollutant in water [2], a key driver of eutrophication [3]. Excessive N can lead

* Corresponding author. School of Karst Science, Guizhou Normal University, Guiyang 550001, China.
E-mail address: fa6897@gznu.edu.cn (Z. Zhou).

https://doi.org/10.1016/j.heliyon.2023.e16262
Received 12 March 2023; Received in revised form 28 April 2023; Accepted 11 May 2023
Available online 16 May 2023

to a deterioration in the quality of the water environment [4], and damage aquatic ecosystems. In water, the main forms of N are nitrate nitrogen (NO_3^-), ammonia nitrogen (NH_3–N), and organic nitrogen (ON). It primarily originates from animal husbandry, pesticides and fertilizers, atmospheric deposition, and human activities [5–8].

Researchers have found that the concentration of N in water is closely related to land use. For example, more N is discharged into rivers from cropland [9] and building land [10], while less N is discharged into rivers from grassland [11] and woodland [12], and woodland can even absorb N from water [13]. N content in water coincides highly in time and space with agricultural activities [6], and the significant seasonal and interannual variation [14] also reflects N is related to land use type. Land is an important resource for socioeconomic development [15]. In karst mountains, where soil erosion is severe while land resources are scarce, resolving the conflict between land use type and N input is key to achieving sustainable development. For this, some researchers have used landscape patterns to study the relationship between land use and N inputs in watersheds (*17*). However, the results of landscape pattern research are uncertain due to the diversity of spatial scales [16]. If the results of the landscape pattern study are applied to land management, it will lead to increased risk of land fragmentation and nitrogen input [17]. In large-scale areas, land use is a factor that causes rapid changes in water quality. For example, water quality deterioration is more severe when the cropland exceeds 50% [18,19]. The coexistence of land types means that the control effect of land use on N input to the watershed becomes complex, and not only the traceability of N affected, but also the transport, migration, and transformation of N [8,10,20].

In karst mountain regions where arable land resources are scarce, research into the appropriate configuration of land use types can not only mitigate the effects of N inputs to the water and provide a scientific basis for guiding water management and land use planning in the watershed, but can also reasonably secure the land resources needed for human life and achieve ecological protection and coordinated socioeconomic development.

2. Materials and methods

2.1. Selection of the study area

We selected the Pingzhai Reservoir Basin as the study area, which is located at the junction of Bijie and Liupanshui cities in Guizhou Province, Southwest China. It is a typical karst peak valley basin with an area of 834.44 km^2, of which 620.01 km^2 is a karst area. The study area includes both mountainous and hilly terrain, with six types of land use (cropland, woodland, grassland, construction land, water, and unused land) (Fig. 1). The Sancha River is the main river in the basin, and its tributaries are the Shuigong, Zhangwei, Baishui, and Hujia Rivers. The Pingzhai Reservoir in the basin is the source water reservoir of the Qianzhong Water Conservancy Hub in Guizhou Province; its water quality is classified as category III. The population of the study area is 339,800, and the per capita arable land is 93.4 m^2, which is far below the national and world averages. The per capita GDP is only 43% of that of Guizhou Province, and

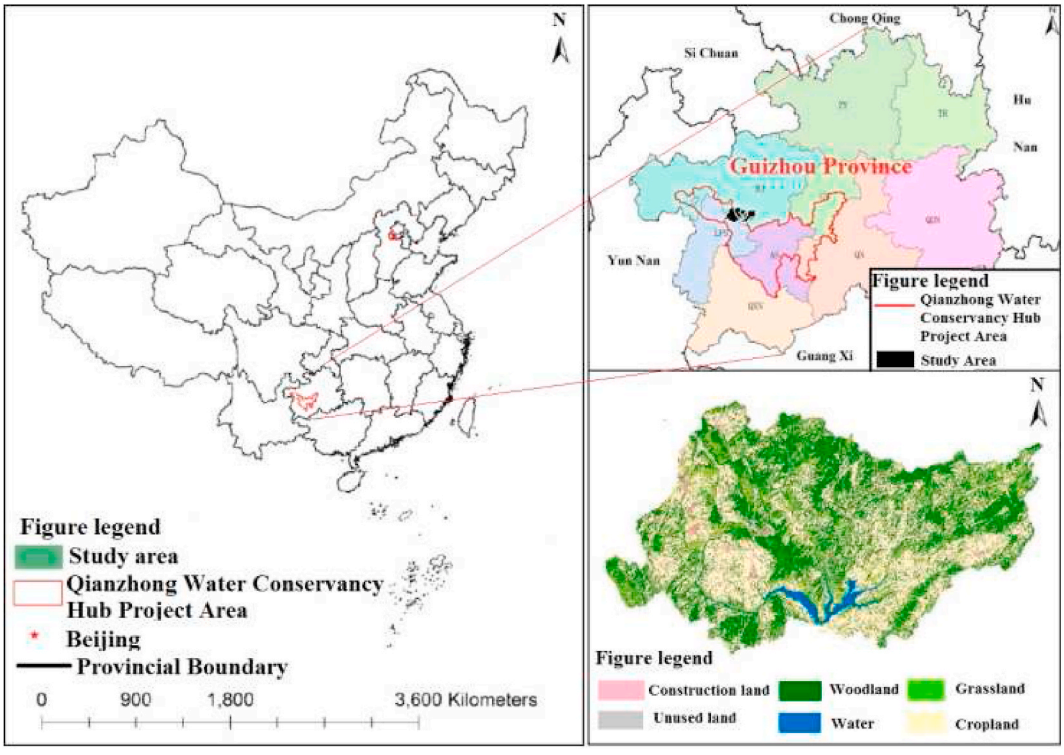

Fig. 1. Location map of the study area.

the conflict between people and land is pronounced. From 2015 to 2021, the land types in the study area changed significantly due to the construction of the project [21]. These conditions in the study area may provide good conditions for establishing the relationship between land use change and N input.

2.2. Sampling and analysis

Eight sampling sites (NY, SG, SG1, HJ, ZW, BS, PZ, PZ1) were established in the study area to analyze water quality and eutrophication according to the hydraulic connection and the river confluence (Fig. 2). These sites were all located on the midline and 0.1 m below the water surface. NY, SG, HJ, ZW, and BS represent the water quality and pollution status of the five tributaries in the catchment, respectively. SG1 represents the water quality status after the confluence of the Zhang Wei, Baishui, and Hujia Rivers. PZ1 represents the water quality status after the confluence of all five tributaries, and PZ represents the water quality status of the reservoir [22].

From January 2015 to December 2021, the study measured pH (±0.01), dissolved oxygen concentration (DO; ±0.01 mg L^{-1}), permanganate index (COD_{Mn}; ±0.1 mg L^{-1}), chemical oxygen demand (COD; ±0.01 mg L^{-1}), five-day biochemical oxygen demand (BOD_5; ±0.1 mg L^{-1}), ammonia nitrogen (NH_3–N; ±0.01 mg L^{-1}), total nitrogen (TN; ±0.01 mg L^{-1}), total phosphorus (TP; ±0.001 mg L^{-1}), total copper (Cu; ±0.001 mg L^{-1}), total zinc (Zn; ±0.001 mg L^{-1}), cadmium (Cd; ±0.0001 mg L^{-1}), lead (Pb; ±0.001 mg L^{-1}), fluoride (F^-; ±0.01 mg L^{-1}), hexavalent chromium (Cr^{6+}; ±0.001 mg L^{-1}), arsenic (As; ±0.001 mg L^{-1}), mercury (Hg; ±0.00001 mg L^{-1}), selenium (Se; ±0.001 mg L^{-1}), cyanide (CN^-; ±0.0001 mg L^{-1}), volatile phenols (Ar-OH; ±0.001 mg L^{-1}), petroleum, animal fats and vegetable oils (Oil; ±0.001 mg L^{-1}), anionic surfactant (LAS; ±0.01 mg L^{-1}), sulphones (S^{2-}; ±0.01 mg L^{-1}), transparency (SD; ±0.1 m), and faucal coliform group (FCG; ±10 L^{-1}) at each sampling site. During sampling, DO and pH were measured using the Multi 3430 portable multi-parameter water quality analyzer (WTW Co. Ltd, Germany), and SD was measured using a Seier disc. Samples for analysis of COD_{Mn}, COD, BOD_5, NH_3–N, TN, TP, Cu, Zn, Cd, Pb, F^-, Cr^{6+}, As, Hg, Se, CN^-, Ar-OH, Oil, LAS, S^{2-}, FCG were collected in containers, added preservatives and stored at 4 °C. Samples were analyzed within the expiry date. Details of sampling frequency, containers, preservatives, sample volumes, and analytical methods were given in the Supplementary Table. In this table, all analytical methods are current standards issued by the Ministry of Ecology and Environmental Protection of the People's Republic of China (https://www.mee.gov.cn/ywgz/fgbz).

From November 2018 to December 2021, chlorophyll *a* (chl-a; ±0.001 mg L^{-1}) was measured 15 times at each site. The samples were collected in dark bottles, then added 0.5 ml magnesium carbonate suspension and stored at 4 °C. Samples were analyzed within the expiry date. Details of sampling frequency, containers, preservatives, sample volumes, and analytical methods were given in the Supplementary Table.

In November 2020, January 2021, April 2021, and July 2021, nitrate oxygen isotope ($\delta^{18}O$–NO_3^-) and nitrate nitrogen isotope ($\delta^{15}N$–NO_3^-) were measured at each site. Samples were filtered through 0.25 μm pore size acetate membranes, placed in prewashed 50 ml polyethylene bottles, sealed, stored at 4 °C, and then returned to the laboratory for determination. We first used denitrifying bacteria (ATCC 13985, DSM 6698) to convert NO_3^- to N_2O, and then used Gas-Bench to introduce a continuous flow of gas into the MAT

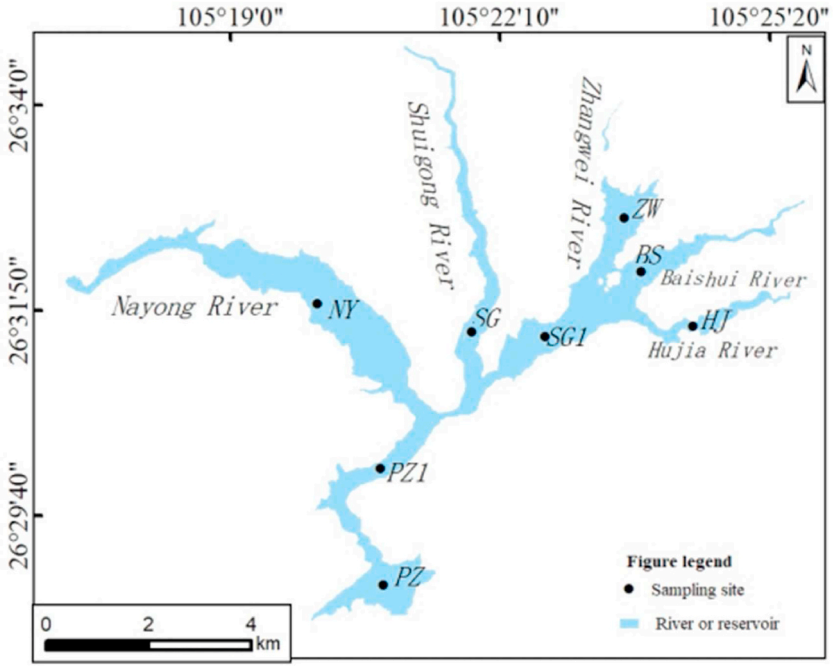

Fig. 2. Location of the sampling point in the Pingzhai Watershed.

253-MS to determine the $\delta^{15}N$ and $\delta^{18}O$ values in N_2O. Standards and blanks were added during the experiment. The precision of the $\delta^{15}N$–NO_3^- and $\delta^{18}O$–NO_3^- was 0.3‰. The $\delta^{15}N$ and $\delta^{18}O$ results were based on atmospheric nitrogen (N_2) and Vienna Standard Average Seawater (V-SMOW) as reference standards, respectively [23]. Samples were analyzed within the expiry date. Details of sampling frequency, containers, preservatives, sample volumes, and analytical methods were given in the Supplementary Table.

2.3. Water quality assessment

The single-factor index (P) method is the most commonly used method in water quality assessment; it can provide a simple and clear understanding of water quality conditions. If $P \leq 1$, the water quality meets the standard, and if $P > 1$, water quality exceeds the standard.

The following equations were used to calculate the single-factor index during the water quality assessment.

(1) Special evaluation mode of pH water quality factor:

$$P_{pH} = \left(pH_j - 7.0\right)/(pH_{su} - 7.0) \ldots\ldots pH_j > 7.0$$
$$P_{pH} = \left(7.0 - pH_j\right)/(7.0 - pH_{sd}) \ldots\ldots pH_j \leq 7.0$$

Where,

pH_{sd} − Lower limit value of pH

pH_{su} − Upper limit value of pH

pH_j − Measuredvalue of pH

(2) DO special water quality factor evaluation mode:

$$SDO_j = \left|DO_f - DO_j\right|/\left(DO_f - DO_s\right) \ldots\ldots \left(DO_j > DO_s\right)$$

$$SDO_j = 10 - \frac{9DO_j}{DOs} \ldots\ldots \left(DO_j \leq DO_s\right)$$

Where,

SDO_j − Standard indices of DO

DO_f − Saturated dissolved oxygen concentration

DO_j − Dissolved Oxygen Measured Values

DOs − Standard limits for the evaluation of dissolved oxygen

(3) Other index evaluation modes:

$$P_i = C_i/S_i$$

Where,

P_i − Pollution index for pollutant ″ i ″;

C_i − Measured value of pollutant ″ i ″, mg/L

S_i − Evaluation criteria for pollutant ″ i ″, mg/L.

2.4. Nutrient status evaluation

The comprehensive nutritional status index of the reservoir was calculated using the following equation:

$$\sum_{j=1}^{5} T_{LI,j} = \sum_{j=1}^{5} W_j \times TLI_{(j)}$$

Where,

$\sum_{j=1}^{5} T_{LI,j}$ − Composite nutritional status index

j − Indicator ″ j ″, $j = 1, 2, 3, 4, 5$;

W_j − Correlation weights of the trophic state index for indicator ″ j ″

$TLI_{(j)}$ − Nutrient status index of indicator ″ j ″

With chl-a as the reference index, the normalized correlation weight calculation formula of the J-th index is as follows:

$$W_j = \frac{r_j^2}{\sum_{j=1}^{5} r_j^2}$$

Where,

W_j − Correlation weight of trophic state index for indicator $''j''$

r_j − Correlation coefficient of the jth indicator with the benchmark indicator chl − a

j − indicator $''j''$

The correlation weights W_j and the correlation coefficients r_j and r_j^2 between chl-a and other indicators of Chinese lakes (reservoirs) are shown in Table 1.

The nutritional status index of each item was calculated using the following equations:

$$TLI_{Chla} = 10 \times (2.5 + 1.086 \times In\rho_{Chla})$$
$$TLI_{TP} = 10 \times (9.436 + 1.624 \times In\rho_{TP})$$
$$TLI_{TN} = 10 \times (5.453 + 1.694 \times In\rho_{TN})$$
$$TLI_{SD} = 10 \times (5.118 - 1.94 \times Ind_{SD})$$
$$TLI_{IMn} = 10 \times (0.109 + 2.661 \times In\rho_{IMn})$$

Where,
TLI_{Chla} − trophic state index of chl − a;
ρ_{Chla} − concentration of chl − a;
TLI_{TP} − trophic state index of TP;
ρ_{TP} − concentration of TP;
TLI_{TN} − trophic state index of TN;
ρ_{TN} − concentration of TN;
TLI_{SD} − trophic state index of SD;
ρ_{SD} − water clarity;
TLI_{IMn} − nutrient status index of permanganate index;
ρ_{IMn} − permanganate index of water.

2.5. Classification of the trophic state of lakes (reservoir)

The trophic status of lakes (reservoirs) was analyzed using a series of consecutive numbers from 0 to 100. If TLI (Σ)<30, it is a oligotrophic lake. If 30≤TLI (Σ)≤50, it is a mesotrophic lake. If 50<TLI (Σ)≤60, it is a slightly eutrophic lake. If 60<TLI (Σ)≤70, it is a moderately eutrophic lake. If TLI (Σ)>70, it is a hypereutrophic lake.

2.6. Interpretation of land use data

Land use data for the study area were obtained from the Sentinel-2 Level-1C product acquired in 2015 and 2021. The data were obtained from the European Space Agency (ESA) data sharing website and had a resolution of 10 m. The data were processed using the Sen2cor atmospheric correction module provided by ESA (http://step.esa.int/main/third-party-plugins-2/sen2cor/), and the radiometric correction of the images was performed using a semi-empirical atmospheric correction method [24]. Based on the needs of the study, land use was classified into six categories: arable land, forest land, grassland, construction land, unused land, and water, initially using unsupervised classification. To improve the accuracy of the interpretation, corrections were made by combining national census data, UAV data, and GPS field survey data, and the overall accuracy of the interpretation reached 90.21%, with a kappa coefficient of 0.85.

3. Results and analysis

3.1. Spatial and temporal changes in the water environment quality in the reservoir

Water quality is an important parameter for determining water use. At present, China mainly uses the single-factor standard index method to evaluate water quality according to the surface water environmental quality standard [25]. The water quality in the

Table 1
Correlation weights r_j, r_j^2 and W_j values among some indicators and chl-a in Chinese lakes (reservoirs).

Indicators	*Chl-a*	TP	TN	SD	I_{Mn}
j	1	2	3	4	5
r_j	1	0.84	0.82	−0.83	0.83
r_j^2	1	0.7056	0.6724	0.6889	0.6889
W_j	0.2663	0.1879	0.1790	0.1834	0.1834

Pingzhai Reservoir and the basin has a P value of less than 1 and is in good condition. TN was evaluated separately, as the above standards did not include TN in the evaluation. From 2015 to 2021, the P values for TN ranged from 0.29 to 5.03, with an exceedance rate of 98.81% and a maximum exceedance multiple of 5.03 times. These results are consistent with the findings from other rivers in the Yangtze River Basin and are mainly attributed to the influence of cultivation, agriculture, and human life [26,27].

Eight monitoring sites were established in the reservoir, and 15 nutrient monitoring sessions were conducted from November 2018 to July 2021. Overall, the reservoir was mesotrophic; it was mildly eutrophic in May and July 2019, and moderately eutrophic in July 2021. The results showed that the Pingzhai Reservoir exhibited a trend of degradation and a tendency to become lacustrine (Fig. 3a), mainly due to the nutrient enrichment as a result of damming. TP and TN were the main factors influencing the trophic state of the water in Pingzhai Reservoir, accounting for 37.04% and 35.87% of the nutrient input, respectively. Combining the results of the single-factor evaluation of the two substances, it is clear that TN is the main pollutant in Pingzhai Reservoir.

3.2. Source and distribution of total nitrogen in Pingzhai reservoir

The concentration of TN in Pingzhai Reservoir and the tributaries exhibit spatial and temporal heterogeneity. TN concentrations were analyzed according to periods of abundance, flat water, and dry water, and it was found that the p-value of the TN content during the abundance period was 0.001 compared to the dry water and flat-water periods, which was highly significant. The p-value for the dry and flat-water periods was 0.079, which was not significant. Thus, the TN content during the abundant water period was significantly higher than that during the dry and flat-water periods (Fig. 3b), indicating that the rainfall cycle has a strong influence on the N-content of the Pingzhai Reservoir watershed, both because rainfall carries atmospheric N into the water and because the scouring of the watershed by rainfall-induced surface runoff is the main pathway for soil and agricultural N to enter the water.

The tributaries in SG had the lowest TN content, whereas those in NY had the highest TN content; the TN concentration value in the

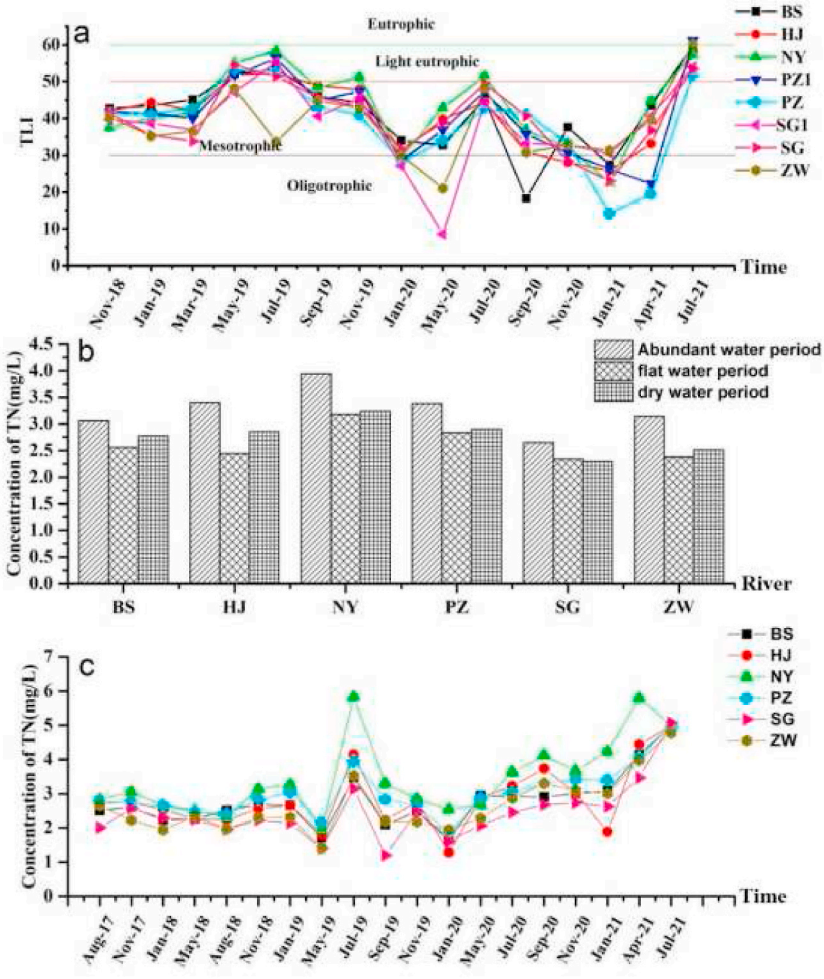

Fig. 3. Results of nutrient status evaluation of Pingzhai Reservoir ("a" is the nutrient status, "b" is the concentration of TN during different water periods, "c" is the concentration of TN during different sampling periods).

reservoir was between those in the tributaries in SG and NY (Fig. 3c). The TN in each tributary was highly significantly and positively correlated with the TN in the reservoir, with their contributions being in the following order: NY > BS > ZW > SG > HJ (Table 2). This showed that TN from the tributaries was the main source of TN in the reservoir and that the reservoir had a mixing effect of the TN from the tributaries.

The concentration of TN gradually increased along with reservoir age, with an overall significant or highly significant positive correlation between TN concentration and reservoir age. TN and reservoir age were not significantly correlated at HJ, and the low contribution of HJ to the reservoir indicated that TN was still mainly of basin origin and that the reservoir had a significant enrichment effect on TN (Table 3).

The concentration of $\delta^{15}N–NO_3^-$ in the Pingzhai reservoir ranged from 0.43‰ to 17.80‰, and that of $\delta^{18}O–NO_3^-$ ranged from −2.05‰ to 23.85‰. The $\delta^{15}N/\delta^{18}O$ ratio indicated that the source of N in the Pingzhai reservoir varied seasonally. In November 2020, the soil was the main source of N. Livestock manure was the main source of N in January and April 2021, and atmospheric deposition was the main source of N in July 2021 (Fig. 4a). The $\delta^{15}N/\delta^{18}O$ ratio in Pingzhai Reservoir varied considerably from one sampling period to another, and the values only fell within the range of 1 or 2 sources for each period.

3.3. Land cover changes in the region

Remote sensing interpretation techniques was used to classify the land use in the 2015 and 2021 images of the Pingzhai Reservoir watershed and to identify the land use changes in the watershed before and after the lower gates of the Pingzhai Reservoir were Constructed. The main land use types in the study area were cropland, woodland, and grassland, with accounting for 92% and 94% of the total area in the target region in 2015 and 2021, respectively. From 2015 to 2021, there were different degrees of changes in each land use type, with the major changes being the changes from cropland to forest land (109.24 km^2) and grassland (49.48 km^2) and the changes from forest land to cropland (92.15 km^2) and grassland (46.89 km^2) (Table 4). By 2021, the proportion of grassland in the Pingzhai Reservoir basin increased from 9.57% to 15.09%, that of woodland increased from 38.32% to 40.33%, and that of water increased from 0.34% to 1.78%, the proportion of cropland decreased from 44.12% to 38.32%, and that of unused land decreased from 3.37% to 0.19%, while the proportion of land for construction remained basically unchanged.

4. Discussion

4.1. Drivers of changes in land use types within a watershed

In the study area, the changes in land use between 2015 and 2021 were significant, with an increase in the area of grassland, woodland, and water, and a decrease in the area of cropland and unused land. The changes in land use were directly or indirectly related to the construction of the reservoir. The reasons for the changes in land use can be summarized: (1) Reservoir storage increased the area of water. (2) Reservoir migration had increased the spatial distance between farmers and their land, increased the cost of farming time and production costs, and, together with the depreciation of farm assets [28], reduced farmers' willingness to farm and increased land abandonment. This is consistent with the results of Wang's analysis of the drivers of arable land decline in China in the 21st century, where higher labor costs lead to a decline in arable land area [29]. (3) Abandoned cropland becomes grassland through a natural evolutionary process. Abandoned cropland evolves in the order of grassland-shrubland-woodland, with the formation of grassland taking only one or two years and the formation of woodland taking about 30 years [30]. The time of the study is only 6 years, so natural evolution is only one of the factors for the increase in grassland area and cannot be a driver for the increase in the woodland area. (4) The function of the Pingzhai reservoir in the watershed is to supply drinking water, and requires strict control of pollutant discharge in the watershed. The implementation of reforestation (grass) policies around the reservoir can stop the inflow of pollutants such as N and P, protect water quality [31], and increase the area of woodland. In other karst areas, such as Huanjiang in Guangxi, the implementation of set-aside and afforestation policies is one of the main drivers of regional land use change [32]. (5) The study area is located in a mountainous area with poorer soil, scattered arable land, and poor irrigation conditions. Farmers in such natural conditions tend to choose non-farm employment [33]. The export of labor has led to labor shortages and the abandonment of cropland in the region. (6) The construction of the reservoir led to the relocation of farmers below the inundation line, unused land was compensated as construction land, and the area of unused land was reduced.

It can be seen that there have been many driving factors for land use change in the Pingzhai reservoir basin and that these factors interact with each other. For example, the construction of a reservoir affects farmers' willingness to farm, natural conditions affect

Table 2
The degree of influence of each tributary on the TN of the watershed.

	PZ	*p*
BS	0.915**	0.000
HJ	0.759**	0.000
NY	0.939**	0.000
SG	0.765**	0.000
ZW	0.899**	0.000

*$p < 0.05$ **$p < 0.01$.

Table 3
Correlation analysis between TN and reservoir age in Pingzhai Reservoir watershed.

River	Reservoir age (months)
BS	0.586**
HJ	0.443
NY	0.584**
PZ	0.594**
SG	0.499*
ZW	0.633**

*$p < 0.05$ **$p < 0.01$.

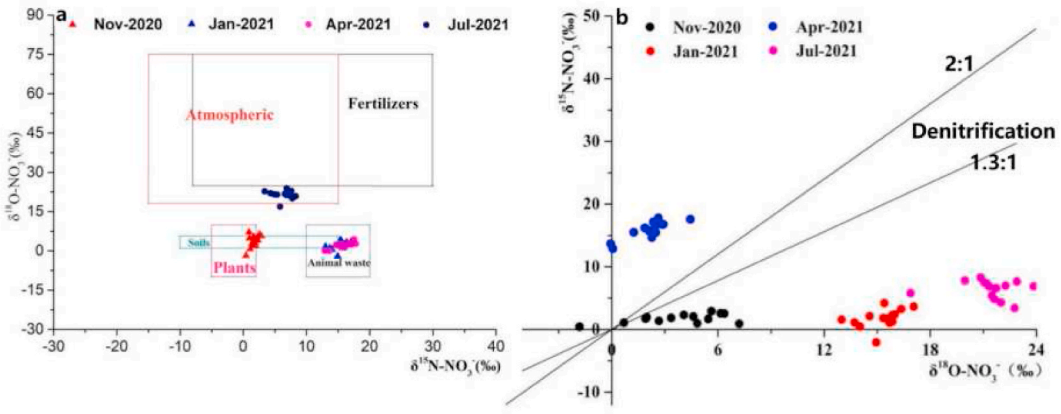

Fig. 4. The Source of N (a) (The $\delta^{15}N$ and $\delta^{18}O$ interval was derived from Kendall (1998)) and judgment of denitrification in Pingzhai Reservoir (b).

Table 4
Land Use Transfer Matrix for Pingzhai Reservoir Watershed, 2015–2021 Unit; km^2.

2015						
2021	Grassland	Cropland	Construction	Woodland	Water	Unused land
Grassland	20.50	18.59	1.34	38.62	0.57	0.23
Cropland	49.48	186.58	17.70	109.24	4.32	0.82
Construction	2.64	13.59	6.57	6.49	6.35	0.07
Woodland	46.89	92.15	9.46	168.43	2.45	0.39
Water	0.46	0.63	0.16	0.61	0.95	0.03
Unused land	5.94	8.19	0.58	13.13	0.20	0.06

farmers' employment choices, and policies to protect drinking water lead to policies to return farmland to forest. In the study of the drivers of land-use change in karst areas, reforestation, and ecological migration [32], poverty alleviation projects [34], continued urban expansion and large-scale planting of economic fruit trees [35], and improvements in agricultural technology [29] are all drivers of land-use change. However, the degree of influence of individual factors varies considerably from region to region. Overall, engineering and policy factors in the Pingzhai Reservoir watershed are the main drivers of land-use change in the watershed.

4.2. Nitrogen source analysis -based on the source-flow-sink research framework

NO_3^- is prone to denitrification during transport [36], so a source-sink approach to tracing is likely to overlook changes in transport, leading to increased uncertainty in tracing results [37]. In this study, the source-stream-sink framework [38,39] was used to fully account for changes during migration processes, which yields more credible results. N in the Pingzhai Reservoir watershed is mainly in the form of inorganic nitrogen, with NO_3^- accounting for 15–70% of the TN concentration. This is consistent with the pattern of N present in most water bodies [40]. Therefore, nitrate was used as a proxy to analyze N migration and transformation in the basin. The DO concentrations in the basin ranged from 6.39 to 15.3 mg L^{-1}, which did not meet the environmental conditions for denitrification to occur. Furthermore, the ratio of $\delta^{15}N$–NO_3^- to $\delta^{18}O$–NO_3^- was not in the range of 1.3–2.0 (Fig. 4b). The average flow velocity of the rivers was 0.42 m/s, which was not conducive to the occurrence of biogeochemical changes in solutes [41]. Thus, the nitrate-nitrogen did not change during transport; this result is consistent with the results of a study in the Yuan Jiang watershed [42].

The $\delta^{15}N/\delta^{18}O$ ratios in the Pingzhai reservoir indicated that the sources of N were livestock manure, atmospheric deposition, and

soil, which were in agreement with the sources calculated using the Bayesian isotope mixing model [23]. In addition, the sources did not exceed the nitrate end elements in the basin identified in previous studies, such as soil, livestock manure or domestic wastewater, and atmospheric deposition [23,43]. The sources in the Pingzhai Reservoir were concentrated in one or two source value intervals during different sampling periods, which is also in good agreement with the results of previous studies [44,45]. Nitrate-nitrogen did not change during transport, but nitrogen is produced at the source by the nitrogen fixation, assimilation or mineralization, after which it undergoes isotopic fractionation and changes its original isotopic fingerprint [34,46,47]. However, in this study, the corresponding isotopic analysis of N sources in the study area was not carried out, so the influence of isotopic fractionation on the traceability results cannot be eliminated.

4.3. Influence of land use change on N inputs

Analysis of the correlation between land use and N-containing substances in the Pingzhai Reservoir watershed shows that land use changes affect N input patterns. In 2015, construction land and water area significantly influenced the input of NH_3–N. In 2021, unused land significantly influenced the input of NH_3–N and NO_2^-, and built-up land significantly influenced the input of NO_2^- (Table 5). The results of the correlation analysis fully reflect the type and intensity of human activities on different lands in the study area. The human activities on the construction land and water bodies are human settlements and fishing, which are the main sources of NH_3–N [48,49]. The change in the correlation between land use and N input in 2015 and 2021 could be explained by the fact that environmental management controls the input of NH_3–N from construction land and water area, but it was also related to the creation of conditions for NH_3–N oxidation to NO_2^- by damming [50].

Unused land was found to have a significant influence on NH_3–N and NO_2^- inputs, a finding that was not mentioned in other studies. However, some studies have mentioned that controlling the proportion of unused land can reduce the emission of pollutants [51]. The unused land lacks management and often becomes a rubbish dump or is temporarily used as a breeding ground. Agricultural drainage, landfill leachate, and human and animal wastes are just the main sources of NO_2^- [52]. It can be seen that although the area of unused land in the study area was small, it could become a new key area for N emissions due to poor environmental management.

In the study area, there was no significant relationship between N inputs and cropland, woodland, and grassland (Table 5). This differed from previous studies, which showed a significant correlation between cropland and N inputs [9], and inhibition of N inputs by woodland and grassland [11,12]. However, the correlation between grassland and $\delta^{15}N$–NO_3^- and the correlation between built-up land and $\delta^{18}O$–NO_3^- suggest that grassland and built-up land are involved in the N cycle in the watershed, but the inhibition of grassland on N may be offset. In karst mountainous areas, when N and P inputs are influenced by cultivated land, the changing trends of both are the same [53], but the changing trends of N and P in the study area from 2015 to 2021 were opposite (Fig. 5), and the effect of cropland on N was weakened. As early as the end of the 20th century, it was confirmed that in the basin where multiple land types coexist, the promoting effect of cropland on N inputs to the basin may be offset by the inhibiting effect of forest land [54]). In the study area, forest land and grassland were classified as ecological land, and cropland and construction land were classified as productive land. The ratio of (ecological land/production land) was 0.98 and 1.28 in 2015 and 2021, respectively, explaining 59.9% and 17.6% of TN sources in the basin, indicating that a high proportion of ecological land can significantly reduce N inputs to the watershed. This is supported by

Table 5
Correlation analysis of land use type and nitrogen content.

Years	Indicators	Correlation analysis	Grassland	cropland	woodland	construction	water	unused land
2015	TN	Correlation coefficient	−0.235	0.217	−0.608	0.486	0.462	0.75
		p	0.704	0.726	0.277	0.407	0.434	0.145
	NH_3–N	Correlation coefficient	0.641	−0.590	−0.181	0.888*	0.900*	0.394
		p	0.243	0.295	0.771	0.044	0.038	0.511
2021	TN	Correlation coefficient	0.325	0.009	−0.271	0.723	−0.197	0.959*
		p	0.594	0.989	0.659	0.167	0.751	0.010
	NH_3–N	Correlation coefficient	0.160	−0.005	−0.241	0.862	0.049	0.996**
		p	0.798	0.994	0.697	0.060	0.937	0.000
	NO_3^-	Correlation coefficient	0.500	−0.024	−0.234	0.510	−0.464	0.831
		p	0.391	0.970	0.705	0.380	0.432	0.081
	NO_2^-	Correlation coefficient	−0.093	−0.062	−0.118	0.973**	0.292	0.911*
		p	0.882	0.922	0.850	0.005	0.634	0.032
	PTN	Correlation coefficient	0.764	−0.675	0.680	−0.754	−0.559	−0.505
		p	0.133	0.212	0.206	0.141	0.327	0.385
	PON	Correlation coefficient	0.759	−0.676	0.683	−0.755	−0.553	−0.51
		p	0.137	0.210	0.203	0.140	0.333	0.381
	DTN	Correlation coefficient	0.778	−0.687	0.685	−0.737	−0.562	−0.481
		p	0.121	0.200	0.202	0.156	0.324	0.412
	DON	Correlation coefficient	0.747	−0.582	0.605	−0.814	−0.687	−0.561
		p	0.147	0.303	0.279	0.094	0.200	0.325
	$\delta^{15}N$–NO_3^-	Correlation coefficient	−0.905*	0.756	−0.547	−0.102	0.600	−0.418
		p	0.034	0.139	0.340	0.870	0.285	0.484
	$\delta^{18}O$–NO_3^-	Correlation coefficient	0.143	0.255	−0.128	−0.915*	−0.396	−0.744
		p	0.819	0.679	0.837	0.029	0.510	0.150

*$p < 0.05$ **$p < 0.01$.

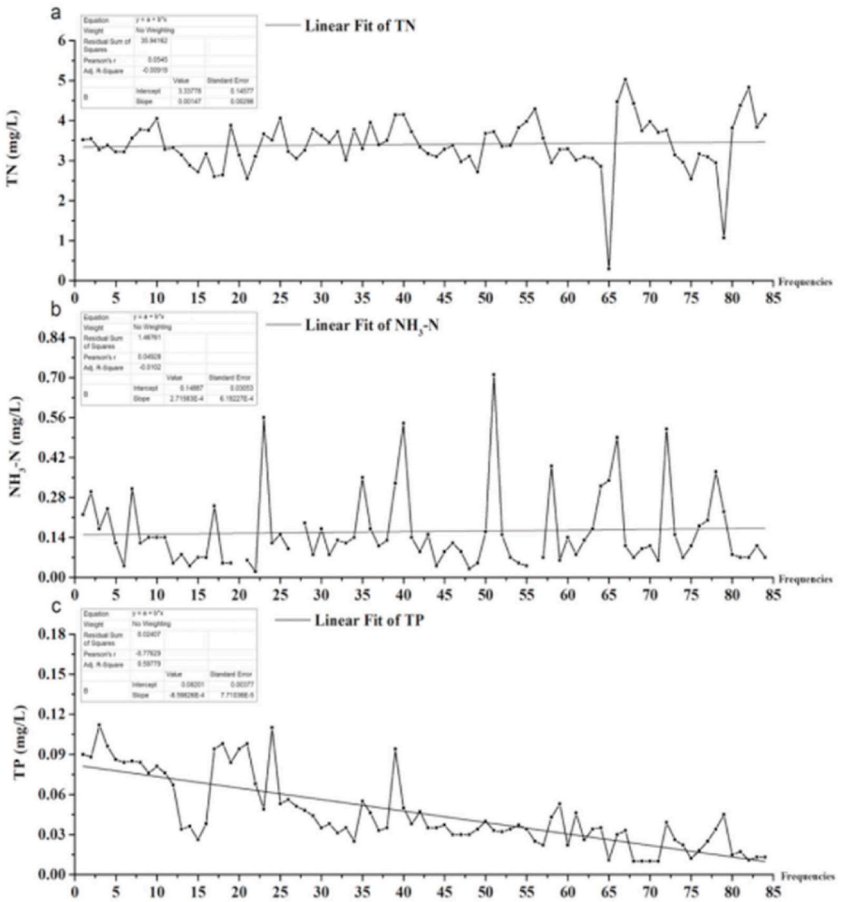

Fig. 5. Trends of TP, TN, and NH_3–N in the Pingzhai Watershed during 2015–2021. ("a" is the change trend of TN, "b" is the change trend of NH_3–N and "c" is the change trend of TP).

the conclusion that more than 50% of cropland can cause a sudden deterioration in water quality [18,19]. The results suggest that optimizing the proportion of cropland, woodland, grassland, and construction land in a watershed can effectively control N inputs. However, the effect of topography, rainfall and transfer distance on N inputs was not considered in this study. Therefore, the above factors need to be considered to extend the conclusion to karst mountain areas for application.

5. Conclusion

(1) The water quality of Pingzhai Reservoir is generally good, TN is the main pollutant, and the reservoir has an enrichment effect on TN. Nitrate nitrogen is the main form of N in the Pingzhai Reservoir, and denitrification does not occur during the migration process. The sources of N are soil, livestock manure or domestic sewage, and atmospheric deposition. The main sources of N in the Pingzhai Reservoir vary seasonally, with TN levels being significantly higher during periods of abundance than during periods of drought and flat water; rainfall carries atmospheric N, soil N, and livestock effluent into the water column. Isotopic fractionation at the source of N in the Pingzhai Reservoir affects the source traceability of N, so isolating the source influence is the key to improving the accuracy of nitrogen and oxygen isotope traceability results in the Pingzhai Reservoir.

(2) From 2015 to 2021 in the Pingzhai Reservoir basin, the area of grassland increased by 5.52%, that of woodland increased by 2.01%, that of water area increased by 1.44%, that of cropland decreased by 5.80%, that of unused land decreased by 3.18%, and that of construction land remained unchanged. Reservoir construction, depreciation of cropland assets, the willingness of farmers to farm, reforestation, and drinking water protection policies are all factors affecting regional land use change, but policy and reservoir construction are the main drivers of land use change in the study area.

(3) In 2015, construction land and water significantly influenced the input of NH_3–N. In 2021, unused land significantly affected the inputs of NH_3–N and NO_2^-, and construction land significantly affected the input of NO_2^-. Changes in land use structure affect N input patterns, and utilized land is a new key area for N input due to the lack of responsible subjects and inadequate environmental management. The promoting effect of cultivated land and construction land in the watershed on N input to the

watershed is offset by the inhibiting effect of woodland and grassland. Thus, optimizing the proportion of woodland to grassland can significantly reduce N input to the watershed.

5.1. Founding

This work was supported by the National Natural Science Foundation of China (Nos. 42161048), The Science and Technology Foundation of Guizhou Province (QKHJC-Z K [2021]-191).

Author contribution statement

Cui Wang: Conceived and designed the experiments; Performed the experiments; Analyzed and interpreted the data; Wrote the paper.

Zhongfa Zhou: Conceived and designed the experiments; Contributed reagents, materials, analysis tools or data; Wrote the paper.

Yongliu Li: Performed the experiments; Analyzed and interpreted the data.

Jie Kong: Performed the experiments.

Hui Dong: Contributed reagents, materials, analysis tools or data.

Data availability statement

Data will be made available on request.

Declaration of competing interest

The authors declare that they have no known competing financial interests or personal relationships that could have appeared to influence the work reported in this paper.

Appendix A. Supplementary data

Supplementary data to this article can be found online at https://doi.org/10.1016/j.heliyon.2023.e16262.

References

[1] A.P. Räike, S. Rekolainen, P. Kauppila, H. Pitkanen, J. Niemi, A. Raateland, J. Vuorenmaa, Trends of phosphorus, nitrogen and chlorophyll a concentrations in Finnish rivers and lakes in 1975–2000, Sci. Total Environ. 310 (2003) 47–59.
[2] K.Q. Li, et al., Linking water quality with the total pollutant load control management for nitrogen in Jiaozhou Bay, China, Ecol. Indicat. 85 (2018) 57–66.
[3] W.K. Dodds, V.H. Smith, Nitrogen, phosphorus, and eutrophication in streams, Inland Waters 6 (2016) 155–164.
[4] V.H.T. Smith, J.C. Nekola, Eutrophication: impacts of excess nutrient inputs on freshwater, marine, and terrestrial ecosystems, Environ. Pollu. 100 (1999) 179–196.
[5] J.H. Qu, J. Zhou, K. Ren, Identification of nonpoint source of pollution with nitrogen based on soil and water assessment tool (swat) in qinhuangdao city, China, Environ. Eng. Manag. J. 14 (2015) 1887–1895.
[6] Y.X. Yang, et al., Types and distribution of organic amines in organic nitrogen deposition in strategic water sources, Int. J. Environ. Res. Publ. Health 19 (2022).
[7] Z.H. Wang, L. Wan, C.M. Xu, Spectrums of nitrogen and phosphorus leaching loss from different land-use types, Clean-Soil Air Water 46 (2018).
[8] M. Wang, et al., Using dual isotopes and a bayesian isotope mixing model to evaluate nitrate sources of surface water in a drinking water source watershed, east China, Water 8 (2016).
[9] L.Y. Liu, X.Q. Zheng, C.F. Peng, J.Y. Li, Y. Xu, Driving forces and future trends on total nitrogen loss of planting in China, Environmental Pollution 267 (2020).
[10] X. Chen, Y.H. Wang, Z.C. Cai, C.B. Wu, C. Ye, Effects of land-use and land-cover change on nitrogen transport in northern taihu basin, China during 1990-2017, Sustainability 12 (2020).
[11] M.Y. Liu, D.A.N. Ussiri, R. Lal, Soil organic carbon and nitrogen fractions under different land uses and tillage practices, Commun. Soil Sci. Plant Anal. 47 (2016) 1528–1541.
[12] A. Bardule, A. Iital, D. Lazdina, I. Karklina, Z. Libiete, A reactive nitrogen budget for forest land and wetlands in Latvia and Estonia, Scand. J. For. Res. 35 (2020) 513–522.
[13] H.M. Bu, Y. Zhang, W. Meng, X.F. Song, Effects of land-use patterns on in-stream nitrogen in a highly-polluted river basin in Northeast China, Sci. Total Environ. 553 (2016) 232–242.
[14] Y.L. Huang, J.L. Huang, A. Ervinia, S.W. Duan, S.S. Kaushal, Land use and climate variability amplifies watershed nitrogen exports in coastal China, Ocean Coast Manag. 207 (2021).
[15] A.M. Breure, J.P.A. Lijzen, L. Maring, Soil and land management in a circular economy, Sci. Total Environ. 624 (2018) 1125–1130.
[16] J.H. Wu, J. Lu, Spatial scale effects of landscape metrics on stream water quality and their seasonal changes, Water Res. 191 (2021).
[17] L.C. Chiang, Y.C. Wang, Y.K. Chen, C.J. Liao, Quantification of land use/land cover impacts on stream water quality across Taiwan, J. Clean. Prod. 318 (2021).
[18] J.D. Allan, Landscapes and riverscapes: the influence of land use on stream ecosystems, Ann. Rev. Ecol. Evol. Syst. (2004) 257–284.
[19] L. Wang, J. Lyons, P. Rasmussen, P. Seelbach, T. Simon, M. Wiley, P.M. Stewart, Watershed, reach, and riparian influences on stream fish assemblages in the Northern Lakes and Forest Ecoregion, USA, Can. J. Fish. Aquat. Sci. 60 (2003) 491–505.
[20] E. Vogt, et al., Catchment land use effects on fluxes and concentrations of organic and inorganic nitrogen in streams, Agric. Ecosyst. Environ. 199 (2015) 320–332.
[21] C. Zhao, Research on compensation for reservoir land acquisition based on ecological compensation - taking the Qianzhong Water Conservancy Hub Project as an example, J. Southwest Nor. Univer.(Natural Science Edition) 37 (2012) 53–59.

[22] M. o. E. a. E. o. t. P. s. R. o. China, Tate Environmental P, BeiJing, 2002, p. 58, vol. HJ/T 91-2002.
[23] J. Kong, Research on the Source and Estimation of Nitrate in Karst Reservoir Water Based on Nitrogen and Oxygen Isotopes-Taking Pingzhai Reservoir as an Example, MA thesis, Guizhou Normal University, 2022.
[24] Zhou Zhongfa Dan Yusheng, Shaohui Li, Haotian Zhang, Yi Jiang, Retrieval of chlorophyll-a concentration in Pingzhai Reservoir based on sentinel-2, Environ. Eng. 38 (2020) 180–185+127.
[25] Notice on the issuance of the "Surface Water Environmental Quality Assessment Scheme (for Trial Implementation) (Office of the Ministry of Environmental Protection [2011]22, 2011).
[26] Y.R. Zhang, Z.F. Zhou, H.T. Zhang, Y.S. Dan, Quantifying the impact of human activities on water quality based on spatialization of social data: a case study of the Pingzhai Reservoir Basin, Water Supply 20 (2020) 688–699.
[27] J. Zhang, Q.J. Guo, C.J. Du, R.F. Wei, Quantifying the effect of anthropogenic activities on water quality change in the Yangtze River from 1981 to 2019, J. Clean. Prod. 363 (2022).
[28] Yahui Wang Xin Liangjie, Li Xiubin., Characteristics on devaluation of cultivated land and its mechanisms in typical mountainous areas in Chongqing ,China, J. Agr. Eng. 35 (2019) 107–114.
[29] X. Wang, X.B. Li, China's agricultural land use change and its underlying drivers: a literature review, J. Geogr. Sci. 31 (2021) 1222–1242.
[30] M.H. Gu, S.L. Liu, H.C. Duan, T. Wang, Z. Gu, Dynamics of community biomass and soil nutrients in the process of vegetation succession of abandoned farmland in the loess plateau, Front. Environ. Sci. 9 (2021).
[31] W.Z. Wang, et al., Is returning farmland to forest an effective measure to reduce phosphorus delivery across distinct spatial scales? J. Environ. Manag. 252 (2019).
[32] F.Y. Zheng, Y.C. Hu, Y.Q. Zuo, Did the ecological engineering have a great impact on the land use change? Environ. Monit. Assess. 190 (2018).
[33] L.J. Xin, X.B. Li, Changes of multiple cropping in double cropping rice area of southern China and its policy implications, J. Nat. Resour. 24 (2009) 58–65.
[34] B. Zhang, et al., Hydrochemical characteristics of groundwater and dominant water-rock interactions in the delingha area, qaidam basin, northwest China, Water 12 (2020).
[35] Y. Chen, S.Y. Wang, Y.H. Wang, Spatiotemporal evolution of cultivated land non-agriculturalization and its drivers in typical areas of Southwest China from 2000 to 2020, Rem. Sens. 14 (2022).
[36] A.R. Boyer Ew, W.J. Parton, C. Li, K. Butterbach-Bahl, S.D. Donner, R.W. Skaggs, S.J. Del Grosso, Modeling denitrification in terrestrial and aquatic ecosystems at regional scales, Ecol. Appl. 16 (2006) 2123–2142.
[37] P.M. Groffman, et al., Challenges to incorporating spatially and temporally explicit phenomena (hotspots and hot moments) in denitrification models, Biogeochemistry 93 (2009) 49–77.
[38] C.S. Dollar, K.H. Rogers, M.C. Thoms, A framework for interdisciplinary understanding of rivers as ecosystems, Geomorphology 89 (2007) 147–162.
[39] C. Girard, J.D. Rinaudo, M. Pulido-Velazquez, Y. Caballero, An interdisciplinary modelling framework for selecting adaptation measures at the river basin scale in a global change scenario, Environ. Model. Software 69 (2015) 42–54.
[40] B.P. Ganasri, H. Ramesh, Assessment of soil erosion by RUSLE model using remote sensing and GIS - a case study of Nethravathi Basin, Geosci. Front. 7 (2016) 953–961.
[41] T. Kolbe, et al., Coupling 3D groundwater modeling with CFC-based age dating to classify local groundwater circulation in an unconfined crystalline aquifer, J. Hydrol. 543 (2016) 31–46.
[42] L. Yu, T.Y. Zheng, X.L. Zheng, Y.J. Hao, R.Y. Yuan, Nitrate source apportionment in groundwater using Bayesian isotope mixing model based on nitrogen isotope fractionation, Sci. Total Environ. 718 (2020).
[43] Z.J. Li, Q. Yang, C.C. Xie, X.Y. Lu, Source Identification and Health Risks of Nitrate Contamination in Shallow Groundwater: a Case Study in Subei Lake Basin, Environmental Science and Pollution Research, 2022.
[44] S.W. Duan, S.S. Kaushal, E.J. Rosenfeldt, J.L. Huang, S. Murthy, Changes in concentrations and source of nitrogen along the Potomac River with watershed land use, Appl. Geochem. 131 (2021).
[45] A.Q. Zhang, L. Kun, L. Qi, Y. Li, Identification of nitrogen sources and cycling along freshwater river to estuarine water continuum using multiple stable isotopes, Sci. Total Environ. 851 (2022).
[46] O. Nikolenko, A. Jurado, A.V. Borges, K. Knoller, S. Brouyere, Isotopic composition of nitrogen species in groundwater under agricultural areas: a review, Sci. Total Environ. 621 (2018) 1415–1432.
[47] E.P. Minet, et al., Combining stable isotopes with contamination indicators: a method for improved investigation of nitrate sources and dynamics in aquifers with mixed nitrogen inputs, Water Res. 124 (2017) 85–96.
[48] R.S.S. Wu, The environmental impact of marine fish culture: towards a sustainable future, Mar. Pollut. Bull. 31 (1995) 159–166.
[49] C. Sanz-Lazaro, N. Casado-Coy, E.M. Calderero, U.A. Villamar, The environmental effect on the seabed of an offshore marine fish farm in the tropical Pacific, J. Environ. Manag. 300 (2021).
[50] H.N. Wu, et al., Integrating experiments with system-level biogeochemical modeling to understand nitrogen cycling of reservoir sediments at elevated hydrostatic pressure, Environ. Res. 200 (2021).
[51] Z.N. Shehab, N.R. Jamil, A.Z. Aris, N.S. Shafie, Spatial variation impact of landscape patterns and land use on water quality across an urbanized watershed in Bentong, Malaysia, Ecol. Indicat. 122 (2021).
[52] D.A. Parvizishad, A.H. Mahvi, F. Goodarzi, A review of adverse effects and benefits of nitrate and nitrite in drinking water and food on human health, Health Scope 6 (2017), e14164.
[53] X. Zhou, W.B. Zhang, Y. Pei, X. Jiang, S.T. Yang, Zoning strategy for basin land use optimization for reducing nitrogen and phosphorus pollution in Guizhou karst watershed, Water 14 (2022).
[54] W. T. a. C. Peterjohn, D.L., Nutrient dynamics in an agricultural watershed: observations on the role of A riparian forest, Ecology 65 (1984) 1466–1475.